

Research Article

# SMART RHESINs for magnetic particle imaging: impact of viscosity-independent relaxation on image reconstruction

J. Feye<sup>a,b</sup> · J. Franke<sup>c</sup> · J. Treptow<sup>b</sup> · C. Feldmann<sup>b</sup> · P. W. Roesky<sup>b</sup> · E. S. Rösch<sup>a,\*</sup>

<sup>a</sup>Faculty of Engineering, Baden-Württemberg Cooperative State University Karlsruhe, Germany

<sup>b</sup>Institute of Inorganic Chemistry, Karlsruhe Institute of Technology (KIT), Germany

<sup>c</sup>Bruker BioSpin GmbH & Co. KG, Ettlingen, Germany

\*Corresponding author, email: [esther.roesch@dhbw-karlsruhe.de](mailto:esther.roesch@dhbw-karlsruhe.de)

Received 08 November 2024; Accepted 13 February 2025; Published online 26 August 2025

© 2025 Feye et al.; licensee Infinite Science Publishing GmbH

This is an Open Access article distributed under the terms of the Creative Commons Attribution License (<http://creativecommons.org/licenses/by/4.0>), which permits unrestricted use, distribution, and reproduction in any medium, provided the original work is properly cited.

## Abstract

Magnetic particle imaging (MPI) is a promising medical imaging modality that leverages the magnetic properties of nanoparticles. Traditionally, MPI tracers have been limited to commercially available nanoparticles, but specialized tracers could improve signal detection and expand applications. Here, we introduce SMART RHESINs, an innovative tracer design for MPI. In SMART RHESINs, synomag<sup>®</sup>-D nanoparticles are encapsulated in hollow nanospheres, shielding them from external influences like viscosity changes and enabling signal quantification independent of the surrounding medium. We demonstrated that the phase angle obtained through MPS is a rapid, predictive metric for assessing tracer suitability for MPI applications. Unlike the system matrix from non-encapsulated synomag<sup>®</sup>-D, the system matrix from aqueous synomag<sup>®</sup>-D-encapsulated SMART RHESINs allowed reconstructing immobilized SMART RHESINs, underscoring design robustness. SMART RHESINs hold potential for quantitative measurements across diverse environments, broadening the scope of MPS and MPI as a versatile tracer platform for quantitative imaging.

## 1. Introduction

In the ever-advancing field of medical imaging, magnetic particle imaging (MPI) is a pioneering modality that enables deep tissue visualization through a non-invasive, high-resolution imaging technique and leverages the magnetic properties of nanoparticles to improve standards for diagnostics and research in the years to come. Superparamagnetic tracers are required for imaging, and their detection in a field-free point or line (FFP or FFL) enables their 3D encoding and visualization [1]. So far, commercially available core/shell nanoparticles such as synomag<sup>®</sup>, perimag<sup>®</sup> (micromod, Germany) or

Resovist (Bayer Healthcare, Germany) have been readily used due to their superior signal intensity. However, the development of sophisticated tracers specifically designed for MPI offers significant potential for exploiting the intrinsic signal quantifiability and for biomedical applications. An important feature of the MPI technique is the direct quantifiability of the spatial distribution of the signal. The magnetic nanoparticle (MNP) signal scales with the amount of MNPs per voxel [2]. However, the signal can be affected by factors such as particle aggregation or changes in the viscosity of the surrounding medium [2, 3]. Variations in viscosity, for instance, alter the signal response and lead to systematic

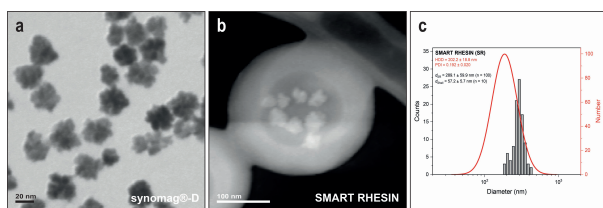


**Figure 1:** Scanning transmission electron microscopy images (STEM) of a) synomag<sup>®</sup>-D, b) of synomag<sup>®</sup>-D-encapsulated SMART RHESIN, and c) particle size distribution of SMART RHESINS based on scanning transmission electron microscopy (STEM) image analysis (SMART RHESIN diameter  $d_{SR}$  and shell diameter  $d_{shell}$ ; histogram in grey) and dynamic light scattering (DLS) (log-normal number-weighted distribution; hydrodynamic diameter (HDD) and polydispersity index (PDI) in red).

errors in quantification. The detected signal is dependent on both, the Brownian (physical rotation of the particle core) and the Néel (rotation of the magnetization vector of the particle) relaxation behavior [4], which are interdependent, especially in core/shell nanoparticles. This interdependence of the two relaxation effects leads to strong signal changes when the tracers are altered or the viscosity of the surrounding medium changes [5, 6]. An MPI-novel nanoparticle design of magnetite-filled hollow nanospheres overcomes these challenges. Herein, we present a novel superparamagnetic magnetite architecture made of phenolic **resin** hollow spheres, referred to as SMART RHESINs (Figure 1). The surface of the SMART RHESINs can additionally be coated with luminescent Eu(III) complex-containing silica nanoparticles as shown previously [7].

## II. Methods

### II.I. SMART RHESIN Synthesis

The method used was previously described by our group [7]. Briefly, sodium oleate (0.089 mmol), Pluronic P123 ( $\text{HO}(\text{CH}_2\text{CH}_2\text{O})_{20}(\text{CH}_2\text{CH}(\text{CH}_3)\text{O})_{70}(\text{CH}_2\text{CH}_2\text{O})_{20}\text{H}$ ) (0.003 mmol) and 250  $\mu\text{l}$  synomag<sup>®</sup>-D70 NPs (micromod, Germany) were blended together with 7 ml deionized  $\text{H}_2\text{O}$  to form mixed micelles. The solution was mixed with 0.45 mmol 2,4-dihydroxybenzoic acid (DHB) and 0.374 mmol hexamethylenetetramine (HMT) and dissolved in 22 ml of deionized  $\text{H}_2\text{O}$  to produce an emulsion. In a 35 ml microwave vessel under hydrothermal condition (150 °C), HMT decomposed and polymerized with DHB on the surface of the micelles, yielding hollow polymer nanospheres containing synomag<sup>®</sup>-D70 NPs. After the microwave reaction, the SMART RHESINs were collected with a magnet, washed with deionized  $\text{H}_2\text{O}$ , and redispersed in 5 ml of deionized  $\text{H}_2\text{O}$  to prepare a stock solution.

### II.II. Magnetic Particle Spectroscopy (MPS)

MPS was measured with a commercial MPS device (MPS-3, Bruker BioSpin GmbH & Co. KG, Germany). An excitation field of  $B_{\text{ex}} = 20\text{ mT}$  and a fixed excitation frequency of  $f_0 = 25.25\text{ kHz}$  was used for all measurements, with data averaging of 10 s. For sample preparation, samples were filled into PCR tubes (MicroAmp<sup>™</sup> Fast Reaction Tube with Cap, 0.1 ml, Applied Biosystems, Thermo Fisher Scientific), using 20  $\mu\text{l}$  sample for each measurement. For immobilization measurements, 20  $\mu\text{l}$  of each NP sample was centrifuged (MiniStar whiteline microcentrifuge, VWR International), the supernatant discarded, and the pellet mixed with 20  $\mu\text{l}$  of a hot (100 °C) agar-agar solution (10 mg/ml) to initiate gelation.

### II.III. Magnetic Particle Imaging (MPI)

MPI measurements were performed using a preclinical MPI system (MPI 25/20 FE, Bruker BioSpin GmbH & Co. KG) installed at Bruker in Ettlingen, Germany. This system is based on the movement of a field-free-point (FFP) through the whole imaging volume, and employs the system function (SF) approach for image reconstruction. Both, system matrix acquisition and image acquisition were performed by setting the strength of the gradient field to 2.5 T/m in the z-direction and 1.25 T/m in the x- and y-directions and the usage of a 1D excitation in the x-direction ( $f_x = 24.51\text{ kHz}$ , of  $B_x = 14\text{ mT}$ ). For the system matrix, a 3D field-of-view (FOV) ( $25 \times 9 \times 9\text{ mm}^3$ ,  $25 \times 3 \times 3$  voxels, averaging = 100) was acquired by means of a robot-based acquisition. For imaging, the respective sample was placed in the center of the FOV with a data acquisition of 21.5 ms duration. Samples were prepared in deionized  $\text{H}_2\text{O}$  (mobile) and 10 mg/ml agar-agar solution (immobilized). For each measurement, 27  $\mu\text{l}$  of sample was used.

### II.IV. Scanning Transmission Electron Microscopy (STEM)

STEM was carried out with a Zeiss Supra 40 VP microscope (Zeiss, Germany), equipped with a Schottky field emitter (2.0 nm resolution). For sample preparation, diluted aqueous suspensions were deposited on amorphous carbon (Lacey-)films (3 nm, 400 mesh) suspended on copper grids (Plano GmbH, Germany, Art. No. 01824) and left for drying at 80 °C for 30 min. The acceleration voltage was in the range of 5-20 kV and the working distance was 2-3 mm. SMART RHESIN diameters were calculated by statistical evaluation of at least 100 nanospheres and analyzed using ImageJ 2.14.0/1.54f software.

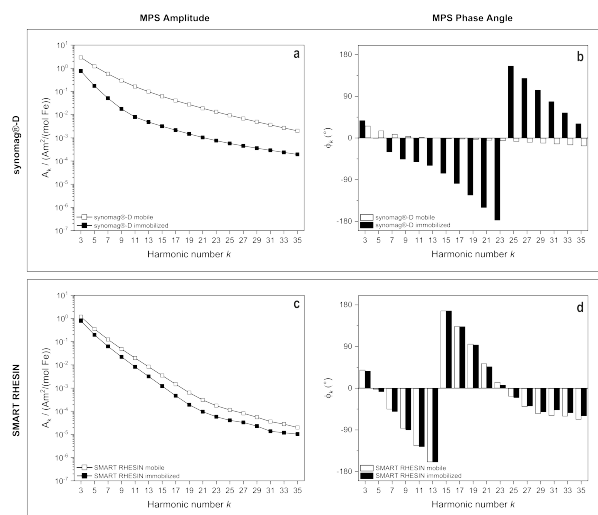


**Figure 2:** MPS amplitudes a) and phase angle b) of synomag®-D mobile (white squares and white bars) and immobilized (black squares and black bars). MPS amplitudes c) and phase angle d) of synomag®-D-encapsulated SMART RHESIN mobile (white squares and white bars) and immobilized (black squares and black bars) at 20 mT and 25.25 kHz. Sample volume 20  $\mu$ l, acquisition time 10 s. The amplitude spectra have been normalized to the iron concentration of the individual samples.

## II.V. Dynamic Light Scattering (DLS)

DLS was performed using a NanoBrook Omni Series analyzer (Brookhaven Instruments, USA) with a 658 nm, nominal 35 mW diode laser to determine hydrodynamic diameter (HDD). Data were processed with Particle Solutions v3.6 software. Samples were measured in polystyrene or quartz glass cuvettes at 25 °C, with a 173° backscatter angle and a dust filter. Each measurement, repeated five times for 3 minutes, provided averaged results. Particle sizes are reported as log-normal number-weighted mean diameters with polydispersity index (PDI), assuming spherical geometry and analyzed using the CONTIN method.

## III. Results and Discussion

Following our previously established protocol [7], synomag®-D was encapsulated in polymeric hollow nanospheres composed of phenolic formaldehyde resin (PFR). This encapsulation shields the synomag®-D nanoparticles from changes in their local environment, such as variations in viscosity. Consequently, the effective relaxation - comprising both Brownian and Néel relaxation - is expected to remain unaffected. To test this hypothesis, magnetic particle spectrometry (MPS) spectra (MPS3, Bruker BioSpin MRI GmbH) of mobile (NPs suspended in water) and immobilized (NPs embedded in agar-agar) synomag®-D and synomag®-D-encapsulated SMART RHESINs were acquired (Figure 2).

For synomag®-D (Figure 2a), the normalized amplitude  $A_k$  of the magnetic moment exhibits a notable difference of approximately one to two orders of magnitude between mobile and immobilized samples, attributed to the altered effective relaxation. Conversely, for the synomag®-D-encapsulated SMART RHESINs (Figure 2c), the amplitude of the magnetic moment for mobile and immobilized samples differs by significantly less than one order of magnitude. The minimal change in the normalized amplitude of SMART RHESINs in Figure 2c might be attributed to negative core coupling resulting from reduced particle distances, which may explain the observed effect. Furthermore, the determination of iron content is known to be prone to significant errors, potentially leading to inaccuracies in its normalization. This explanation appears more plausible, as the phase position remains unchanged - a condition unlikely in the presence of core coupling. Since the synomag®-D nanoparticles are optimized for MPI and exhibit a strong magnetic moment, even small deviations in the iron content of the sample volume can noticeably affect the overall signal. Therefore, minor changes in the iron content during sample preparation could affect the measurement of the immobilized sample. The centrifugation of the nanoparticles to replace the aqueous supernatant with agar-agar likely results in some nanoparticle loss. Given the small measurement volume of 20  $\mu$ l, where hot agar-agar must be pipetted, this could also lead to variations in iron content. An additional determination of iron content was not possible due to the small sample volume. Another potential cause might be that some nanoparticles were not encapsulated during the reaction, potentially altering the signal. However, STEM images (data not shown) collected for statistical analysis of the particle size distribution (Figure 2c) show no free nanoparticles, only encapsulated ones, so we rule out this factor as a cause. However, the phase angles more clearly reveal the differences between the synomag®-D nanoparticles and the encapsulated SMART RHESINs. For synomag®-D, the phase angles differ substantially between mobile and immobilized samples, whereas for the synomag®-D-encapsulated SMART RHESINs, they show only minimal deviation. Stable phase information is crucial in MPI image reconstruction. To demonstrate that the SMART RHESINs provide a consistent environment for overall relaxation, the samples were measured using MPI to investigate whether the SMART RHESINs enable image reconstruction regardless of the viscosity of the surrounding medium. Our study aims to determine whether SMART RHESINs can maintain consistent imaging performance despite variations in viscosity.

For this purpose, for both synomag®-D and SMART RHESINs, one system matrix was acquired in deionized water (i.e., in the mobile state). Subsequently, the mobile and immobilized synomag®-D and SMART RHESIN samples were measured independently and reconstructed

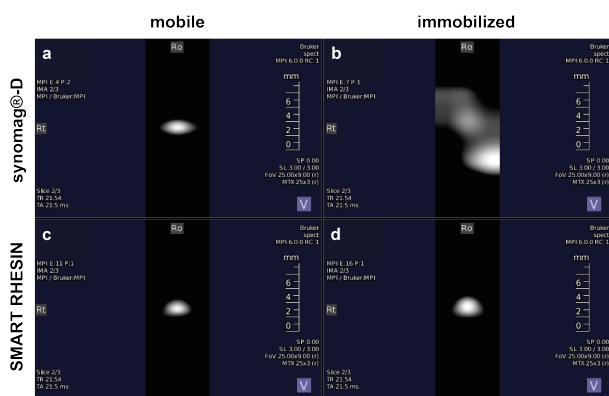


**Figure 3:** MPI image reconstruction of a) synomag®-D mobile and b) synomag®-D immobilized with the system matrix of synomag®-D acquired in deionized water (i.e., mobile). MPI image reconstruction of c) synomag®-D-encapsulated SMART RHESINs mobile and d) synomag®-D-encapsulated SMART RHESINs immobilized with the system matrix of synomag®-D-encapsulated SMART RHESINs acquired in deionized water (i.e., mobile).

using the respective particle specific system matrix. As seen in Figure 3a and c, using the system matrices acquired in aqueous solution can effectively reconstruct the images of the mobile samples. In contrast, for the native synomag®-D nanoparticles (Figure 3b), the system matrix of the mobile synomag®-D fails to detect the immobilized samples (Figure 3b shows an artifact), as the overall relaxation of the synomag®-D nanoparticles has changed significantly due to the substantial increase in viscosity. In MPI, the complex signals are utilized in the reconstruction process. Any changes in relaxation result in alterations to both the magnitude and phase of the harmonics, causing signal localization (i.e., reconstruction) to fail. Therefore, an incorrect phase leads to incorrect imaging or artifacts. In contrast, for the SMART RHESINs, the system matrix from the aqueous sample is capable of reconstructing both the image of the aqueous sample (Figure 3c) and the immobilized sample (Figure 3d). Thus, encapsulating synomag®-D in hollow nanospheres maintains the effective relaxation unchanged regardless of the viscosity of the surrounding medium. Therefore, SMART RHESINs have the potential to enable quantitative measurements in both mobile and immobilized environments using MPS and MPI. Overall, SMART RHESINs represent an exceptional and versatile platform with promising potential for future quantitative applications in medical diagnostics and therapy. Their adaptability to specific medical challenges - whether through the incorporation of different nanoparticles, surface functionalization, polymer modifications, or luminescent labeling - offers a remarkable degree of customization.

## IV. Conclusion

In conclusion, we have successfully demonstrated that synomag®-D nanoparticles - currently recognized for their optimal MPI properties - can be effectively encapsulated in SMART RHESINs. Our results also indicate that MPS measurements, specifically through phase angle analysis, provide a quick and reliable prediction of whether the system matrix can still detect the sample and enable image reconstruction under substantial viscosity changes. SMART RHESINs offer a unique advantage in that they maintain the overall relaxation properties of synomag®-D, allowing robust image reconstruction even under significant viscosity variations. This breakthrough paves the way for quantitative MPI independent of the media conditions, made possible through the novel hollow nanosphere design and performance of these tracers, and holds immense potential for precise and adaptable imaging in biomedical applications. Therefore, the SMART RHESIN approach offers a highly versatile platform to use already established MPI tracers, which is an important aspect of our ongoing research. We are confident that these results will significantly advance the further development of multifunctional theranostic hollow nanosphere tracers, which may also lead to significant advances in both the combination of MPI with magnetic fluid hyperthermia (MFH) and quantitative MPI techniques.

## Acknowledgments

This work was funded by the Deutsche Forschungsgemeinschaft (DFG, German Research Foundation, 363034336 to E.S.R.), supported by the Baden-Württemberg Cooperative State University Karlsruhe Innovation Program Research (IPF) to E.S.R. and a graduate scholarship granted by the State of Baden-Württemberg (Landesgraduiertenförderung to J.Fe.).

## Author's statement

Conflict of interest: Jochen Franke and Julia Feye are employees of Bruker BioSpin GmbH & Co. KG. All other authors declare no conflict of interest.

The authors presented this work under the same title and with the same abstract at IWMPi 2025.

## References

- [1] B. Gleich and J. Weizenecker. Tomographic imaging using the non-linear response of magnetic particles. *Nature*, 435(7046):1214–1217, 2005, doi:[10.1038/nature03808](https://doi.org/10.1038/nature03808).
- [2] J. Rahmer, J. Weizenecker, B. Gleich, and J. Borgert. Signal encoding in magnetic particle imaging: properties of the system function. *BMC Medical Imaging*, 9:4, 2009, doi:[10.1186/1471-2342-9-4](https://doi.org/10.1186/1471-2342-9-4).

- [3] H. Paysen, N. Loewa, A. Stach, J. Wells, O. Kosch, S. Twamley, M. R. Makowski, T. Schaeffter, A. Ludwig, and F. Wiekhorst. Cellular uptake of magnetic nanoparticles imaged and quantified by magnetic particle imaging. *Scientific Reports*, 10(1):1922, 2020, doi:[10.1038/s41598-020-58853-3](https://doi.org/10.1038/s41598-020-58853-3).
- [4] S. A. Shah, D. B. Reeves, R. M. Ferguson, J. B. Weaver, and K. M. Krishnan. Mixed Brownian alignment and Néel rotations in superparamagnetic iron oxide nanoparticle suspensions driven by an ac field. *Physical Review B*, 92(9):094438, 2015, doi:[10.1103/PhysRevB.92.094438](https://doi.org/10.1103/PhysRevB.92.094438).
- [5] M. Möddel, C. Meins, J. Dieckhoff, and T. Knopp. Viscosity quantification using multi-contrast magnetic particle imaging. *New Journal of Physics*, 20(8):083001, 2018, doi:[10.1088/1367-2630/aad44b](https://doi.org/10.1088/1367-2630/aad44b).
- [6] D. Eberbeck, F. Wiekhorst, U. Steinhoff, and L. Trahms. Aggregation behaviour of magnetic nanoparticle suspensions investigated by magnetorelaxometry. *Journal of Physics: Condensed Matter*, 18(38):S2829–S2846, 2006, doi:[10.1088/0953-8984/18/38/S20](https://doi.org/10.1088/0953-8984/18/38/S20).
- [7] J. Feye, J. Matthias, A. Fischer, D. Rudolph, J. Treptow, R. Popescu, J. Franke, A. L. Exarhos, Z. A. Boekelheide, D. Gerthsen, C. Feldmann, P. W. Roesky, and E. S. Rösch. SMART RHESINs—Superparamagnetic Magnetite Architecture Made of Phenolic Resin Hollow Spheres Coated with Eu(III) Containing Silica Nanoparticles for Future Quantitative Magnetic Particle Imaging Applications. *Small*, 19(38), 2023, doi:[10.1002/sml.202301997](https://doi.org/10.1002/sml.202301997).